A bilayer swellable drug-eluting ureteric stent: Localized drug delivery to treat urothelial diseases

Wei Shan Lim[a,f,1], Kenneth Chen[b,1], Tsung Wen Chong[b], Gordon Minru Xiong[a], William R. Birch[c], Jisheng Pan[c], Bae Hoon Lee[a,d,e], Pei Shan Er[a], Abhijit Vijay Salvekar[a], Subbu S. Venkatraman[a,f,+],Yingying Huang[a,f,+]

a School of Materials Science and Engineering, Nanyang Technological University, 50 Nanyang Avenue, Singapore 639798, Singapore

b Department of Urology, Singapore General Hospital, 20 College Road, Singapore 169856, Singapore

c Institute of Materials Research and Engineering, Agency for Science, Technology and Research (A*STAR), 2 Fusionopolis Way, Innovis, Singapore 138634, Singapore

d School of Biomedical Engineering, School of Ophthalmology and Optometry, Eye Hospital, Wenzhou Medical University, Wenzhou 325027, China

e Wenzhou Institute of Biomaterials and Engineering, CNITECH, CAS, Wenzhou 325001, China

f Sino-Singapore International Joint Research Institute, Nanyang Technological University, 50 Nanyang Avenue, Singapore 639798, Singapore

1 First authors. Tel.: +65 9630 1549. E-mail address: ws_lim@live.com (Wei Shan Lim), Tel.: +65 9769 7638. E-mail address: kenneth.chen@singhealth.com.sg (Kenneth Chen)

+Corresponding authors. Tel.: +65 6316 8976; fax: +65 6790 9081. E-mail address: yingyinghuang@ntu.edu.sg (Yingying Huang), assubbu@ntu.edu.sg (S.S. Venkatraman)

Abstract

A bilayer swellable drug-eluting ureteric stent (BSDEUS) is engineered and implemented, as a sustained drug delivery platform technology that enhances localized drug delivery to the highly impermeable urothelium, for the treatment of urothelial diseases such as strictures and carcinomas. On deployment, the device swells to co-apt with the ureteric wall and ensure drug availability to these tissues.

BSDEUS consists of a stent spray-coated with a polymeric drug containing polylactic acid-co-caprolactone (PLC) layer which is overlaid by a swellable polyethylene glycol diacrylate (PEGDA) based hydrogel.

In-vitro quantification of released drug demonstrated a tunable time-profile, indicating sustained delivery over 1-month. The PEGDA hydrogel overlayer enhanced drug release and transport into explanted porcine ureteric tissues *ex-vivo*, under a simulated

dynamic fluid flow. A preliminary pilot *in-vivo* feasibility study, in a porcine model, demonstrated that the swollen hydrogel co-apts with the urothelium and thus enables localized drug delivery to the target tissue section. Kidney functions remained unaffected and device did not result in either hydronephrosis or systemic toxicity.

This successful engineering of a bilayer coated stent prototype, demonstrates its feasibility, thus offering a unique solution for drug-based urological therapy.

Keywords: drug-eluting stent; urological diseases; hydrogel; localized delivery

1. Introduction

The human ureter is a dynamic tubular structure that conveys urine from the kidney to the bladder. Upper tract urothelial carcinomas and strictures, either iatrogenic or lithogenic in nature, form the two most common disease states that plague the ureter. The current standard of care for both conditions is endoscopic surgery, usually with laser energy devices. However, surgical treatment is currently imperfect and has sparked strong interest for adjuvant drug delivery systems in the upper urinary tract to improve treatment outcomes for both conditions.

In low-risk upper tract urothelial carcinoma, organ-preservation with endoscopic treatment is an option; however recurrences are common and for high risk cases of carcinoma-in-situ occurring in the ureter, there is a dearth of optimal methods for drug delivery. Current methods of retrograde bolus instillation of chemotherapy and immunotherapy agents into the bladder are sub-optimal: Yossepowitch *et al.* [1] demonstrated that only 59% of patients have adequate vesico-ureteric reflux hence it is difficult to rely on clinical intravesical chemotherapy for bladder cancer treatment to manage carcinoma in the upper tract. Percutaneous antegrade instillation through the kidney on the other hand causes significant patient morbidity.

Ureteric strictures are highly prevalent in cases of stone disease. Between 14 to 24% of patients with impacted ureteric stones develop post-operative ureteric strictures[2]. Re-stricture rates after endoureterotomy can be as high as 47%[3], prompting utilization of adjuvant topical anti-fibrotic agents such as mitomycin C, a drug which has been in clinical use with encouraging results to mitigate the fibroblastic reaction in esophageal and urethral strictures[4, 5].

The unmet challenges with the current treatment and management of these diseases have prompted the urology community to innovate in the area of ureteric stent, particularly in its drug-eluting stent (DES) technology. Ureteric stents are commonly polyurethane-based tubular scaffolds placed within the ureter post-surgery to facilitate ureteric dilation and healing. These stents are commonly inserted by the urologist

during surgery, and removed easily from the bladder via a cystoscope in the clinic weeks later.

The use of ureteric DESs follows the same concept as those used in coronary vessels[6-10]; The drug-eluting platform coated on the stent allows a controlled release of drugs which limits the fibro-proliferative reaction and potentially minimizes re-stenosis rates in the ureter[11]. Some examples include Urogen Pharma's thermo-reversible hydrogel[12] that produces mitomycin C and Boston Scientific's Lexington® ketorolac-eluting stent and Triumph® triclosan-eluting stent which aim to alleviate stent-related symptoms such as pain and biofilm formation, respectively[13, 14]. In addition, A.A. Barros *et al.* reported on a biodegradable drug-eluting ureteric stent for the treatment of upper tract carcinoma[15-17]. However, to date, there has not been any commercially available drug-eluting ureteric stents on the market.

It is speculated that a major challenge for optimum localized delivery of chemotherapeutics in the ureter is to do with the dynamic nature of fluid flow in the lumen as well as the high drug impermeability of the urothelium. In contrast to the bladder which functions mainly as a reservoir, the ureter serves as a dynamic conduit for the transport of urine which is continuously produced by the kidney. Drug delivery is impeded by a small calibre of the ureteric lumen (3 – 5 mm internal diameter) with regular antegrade peristaltic waves that render constant stable contact with any stent-based drug delivery platform impossible. In addition, the constant flow of urine within the ureter dilutes and washes away any drug being eluted from the stent. In addition, the urothelium comprising of three layers: a basal cell layer attached to a basement membrane, an intermediate layer, and a superficial apical layer with large hexagonal cells (diameters of 25–250 μm), makes it one of the most impermeable membrane barriers in the human body. A synergy of tight junctions, uroplakin plaques, and a dense layer of glycosaminoglycan (GAG) on the apical surface confers resilience and impermeability to the urothelium, rendering it difficult for substances to pass [18-22].

There is no available clinical technique in practice that can deliver therapeutic agents locally to the targeted sites in the urinary tract with significant challenges to deliver drugs across the highly impermeable urothelium. However, studies have shown that the increase of drug residence time on the urothelium can enhance the drug permeation and augment treatment efficacy [23]. Drug eluting balloons (DEBs) are emerging as alternatives to drug-eluting stents (DES) in the field of interventional cardiology[24, 25]. For instance, Liatsikos *et al.* demonstrated that a drug-eluting balloon could enhance the delivery of paclitaxel through the urothelium following 12 hours of close contact between the inflated device surface and tissues [26].

Herein, we propose a novel bilayer swellable hydrogel-based drug-eluting ureteric stent which aims to deliver the drug of interest locally to the desired ureteric diseased site in a

sustained manner over the indwelling stent duration, which may be as long as 4 - 6 weeks, to treat urothelial diseases. The bilayer coatings, that are applied on a bare polyurethane ureteric stent, comprise two layers: a biodegradable polymer (70/30 poly-L-lactide-co-caprolactone, PLC) loaded with a model anti-proliferative drug mitomycin C (MMC) and a layer of hydrogel, polyethylene glycol diacrylate (PEGDA) (Fig i). It is expected that the drug is released from the PLC coating in a sustained fashion and transported across the hydrogel coating to the urothelium as the hydrogel swells upon urine absorption and achieves stable apposition with the ureteric wall for as long as the stent remains in-situ. The hydrogel is necessary for two reasons. Firstly, the hydrogel closes up any possible gap distance between the stent surface and the urothelium as the ureter is commonly wider (3 - 4 mm inner diameter in the middle section) than the stent (1.6 - 2.3 mm outer diameter) and so enables the drug to diffuse laterally across the hydrogel into the tissues before being washed away by the urine flow. Secondly, the co-aptation of the hydrogel with the urothelium helps to extend the drug residence time on the targeted diseased site thereby enhancing the transfer of the drug through the urothelium of high permeability barrier. We hypothesize that this novel technique of drug elution from an indwelling ureteral stent will find useful clinical application in treating both benign ureteric strictures as well as malignant diseases in the ureter.

Even though commercially available ureteric stents such as Cook Medical Universa® Soft stent may have a hydrophilic coating made of hydrogel, this coating does not swell as the dimension remains constant before and after contacting with water. Such coating is usually made of poly vinyl alcohol (PVA) and when hydrated, becomes lubricious to ease the stent implantation procedure by reducing friction [27, 28].

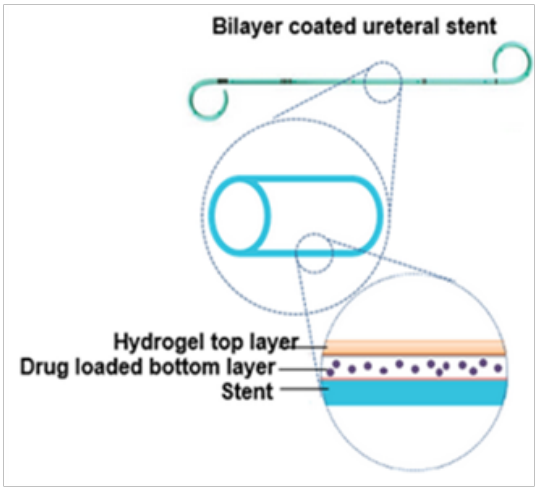

Fig i. ***Schematic diagram for bilayer coated ureteric stent***

2. Materials and methods

2.1 Materials

Polyurethane double pig-tailed ureteric stent (Universa® Soft) was purchased from Cook Ireland Ltd (Limerick, Ireland). Mitomycin C was purchased from Euroasian Chemicals Pte Ltd (Mumbai, India). 70/30 Poly-L-lactide-co-caprolactone (PLC) (Mw 202 000 g/mol) was purchased from Purac Biochem BV (Gorinchem, The Netherlands). The numbers following the copolymer represent the molar ratio of L-lactide/caprolactone monomers respectively. Poly(ethylene glycol)-diol (PEG-OH), acryloyl chloride, phosphate buffer saline tablets (PBS, pH = 7.4), and Irgacure-2959, also known as 2-hydroxy-1-[4-(hydroxyethoxy)phenyl]-2-methyl-1-propanone, were purchased from Sigma-Aldrich (Singapore, Singapore). Primary human bladder stroma fibroblasts (HBdSF), fibroblast basal media, fibroblast growth supplement (FGS) (1% v/v), fetal bovine serum (FBS) (2% v/v) and penicillin/streptomycin (1% v/v) were purchased from Sciencell Research Laboratories (CA, USA). The ultraviolet (UV) lamp (365 nm, 4-5 mW/cm^2) was purchased from Vilber Lourmat (Paris, France).

2.2 Preparation and characterization of hydrogels

Polyethylene glycol diacrylate (PEGDA) was synthesized from the reaction between PEG-OH and acryloyl chloride in an anhydrous condition[29]***(Refer to Supplementary Section, Part I)***. Photocross-linking of PEGDA hydrogel was performed[30] by dissolving PEGDA powder in deionized (DI) water to make either 5%, 7.5% or 10% w/v solution and the Irgacure-2959 photo-initiator in ethanol was added to the PEGDA solution (0.1% w/v). This mixture was exposed to UV-irradiation for 10 min (365 nm, 4-5 mW/cm^2) and immersed in deionized (DI) water overnight to remove any unreacted PEGDA chains and photo-initiator. The hydrogels were then dried in vacuum oven at 37^oC for 1 week to evaporate all the water content before being individually immersed in vials containing phosphate buffer saline (PBS, pH = 7.4). These vials were incubated at 37^oC and samples removed for characterization at different pre-determined time points over a 4-week study. Equilibrium water content and swelling ratio were derived to evaluate the swelling property while mass loss and oscillatory rheological analysis of elastic (storage) modulus measured to evaluate degradation.

2.2.1 Equilibrium water content (%) and swelling ratio

To assess the equilibrium water content (%) and the swelling ratio, the samples were removed from PBS solution at different time points, the surface water on the hydrogel wiped off, and the wet mass (W_{wet}) wasrecorded. The dry mass (W_{dry}) was also recorded initially.

Equilibrium water content, W_{eq} (%) is calculated by: $W_{eq} = \frac{W_{wet} - W_{dry}}{W_{wet}} \times 100$ *(1.1)*

Swelling ratio, Q is calculated as: $Q = \frac{W_{wet} - W_{dry}}{W_{dry}}$ *(1.2)*

2.2.2 Mass loss

For the mass loss measurement, after the samples were taken out at the respective time point, they were rinsed with water to remove PBS salts and then dried in vacuum oven at 37^{o}C for 1 week before the final dry masses (W_t) were recorded and then compared with the initial dry weights (W_0).

Mass loss, M_o is calculated as: $M_o = \frac{W_0 - W_t}{W_0} \times 100$ *(1.3)*

2.2.3 Storage modulus

The oscillatory rheological analysis was performed with rheometer (Anton Paar Physica, MCR 501) using a 10 mm parallel plate geometry to obtain the elastic (storage) modulus of the hydrogels (2 mm height × 6 mm width). Frequency-sweep measurements were performed at 2% strain amplitude and at an oscillation frequency of 0.1 - 5 Hz within the linear viscoelastic region. All test samples were tested only after the hydrogel swelling attained equilibrium state.

2.3 Preparation and characterization of bilayer coated stent prototype

The fabrication method of bilayer coated stent is described in the Patent “A stent assembly and method of preparing the stent assembly” (WO2016/148648)[31]. The method is briefly described here. For the first layer, varying amounts of 70/30 Poly-L-lactide-co-caprolactone (PLC) pellets and mitomycin C (MMC) were dissolved in dichloromethane and stirred continuously overnight until homogeneous polymer solutions were obtained. The drug/polymer solution was coated onto the stent section with a spray-coater (Sono-tek Corporation, MediCoat I) at a constant flow rate of 0.05 mL/min[32]. The stents were transferred into the 37^{o}C vacuum oven for 7 days.

For the second layer, following the coating of the first layer of drug/polymer, the stent was plasma-treated with oxygen for 5 min at power = 100W (Femto Science, Covance-2MP/RF) to impart wettability to the surface before an additional layer of hydrogel was coated on the stent via UV-irradiated photo-crosslinking method with the use of a customized plastic tubing mold (6 mm outer diameter) ***(Refer to Supplementary Section, Part II)***[30]. The hydrogel-coated section herein can swell up to 7 mm in outer diameter after 1 day immersion in phosphate buffered saline (PBS, pH = 7.4) at 37^{o}C and remain constant even after continuous exposure to PBS over 28 days; The size of the coating can be tuned by varying the diameter of the plastic tubing mold.

Thermogravimetric Analyzer TGA (TA Instruments Q500) results showed less than 1 wt% residual solvent.

2.3.1 Surface morphology and cross-section analysis

The surface morphology of the coated stent was analyzed by SEM (JSM, 6360, Tokyo, Japan) at 5 kV before and after release study. The test samples post-study was first rinsed with water to remove PBS salts and then dried completely before analysis.

2.3.2 Static water contact angle measurement

To assess the improvement of surface hydrophilicity due to plasma treatment, PLC was spin-coated onto glass slide for contact angle measurements. PLC (1% w/v) was dissolved in DCM homogenously overnight before the solution (50 µL) was drop-casted onto a slide measuring 1 × 1 cm, using a spin-coater (Sawatec) rotating at 4000 rpm. The coated slides were dried in 37^{o}C vacuum oven for 7 days.

The spin-coated films were then treated with plasma (Femto Science, Covance-2MP/RF) using oxygen at a flow rate of 30 sscm, 100 W and at varying plasma times. The surface was then characterized for wetting properties with Contact Angle (Data Physics) using distilled water. A control was also assessed where no plasma was performed. All samples were evaluated in sets of five (n = 5).

2.3.3 Atomic Force Microscopy (AFM)

Atomic force microscopy was carried out to investigate the effect of plasma treatment times on surface roughness. The surface topography of the plasma-treated spin-coated samples was analyzed using a Nanoscope IIIa Atomic Force Microscope (AFM) (Digital Instruments, Santa Barbara, CA). The images were captured in the tapping mode with the use of monolithic silicon NCH-50 Point Probe (NanoWorld AG, Neuchatel, Switzerland). The scan size was set at 15 × 15µm and the surface was scanned at the rate of 1 Hz using 256 × 256 pixels of resolution. Surface roughness measurements (RMS value) and the 3-dimensional topographical images were recorded using Nanoscope image processing software version 5.12r5 (Digital Instruments). 5 sets of measurements were done for each plasma time (n = 5).

2.3.4 X-ray Photoelectron Spectroscopy (XPS)

XPS measurements were performed on the drug-and-PLC coated stents to evaluate the effect of plasma treatment times on the surface oxidation. Measurements were carried out in a Thermo Fisher Scientific Theta Probe system equipped with a monochromatic, micro-focused Al Kα (1486.6 eV) X-ray source and XPS spectra were recorded at a detection angle (θ) of 50°, with respect to the sample surface. The spectra were analyzed using the Avantage software, combining Gaussian (70%) and Lorentzian

(30%) line shapes and subtracting the secondary electron background with a Shirley function. The lowest number of component spectra was used to obtain acceptably low residual values. Quantitative analysis, including element/bond ratio determination, was achieved using relative sensitivity factors and algorithms embedded in the Avantage software. To eliminate any positive charge induced binding energy shift, besides a low energy electron flood gun was used for charge compensation during spectrum acquisition, the XPS spectra reported here are referenced to C 1s at 285.0 eV.

2.3.5 Shear adhesion delamination test

Shear adhesion failure analysis experiment was conducted to elucidate the effects of plasma treatment on interfacial adhesion. 5 sets of measurements were done for each plasma time (n = 5).

After the drug-and-PLC coated stents were plasma treated, they were placed in a tubing mold. A steel rod was placed within the hollow stent lumen and mounted onto a rubber support while one end of the stent was clamped by a customized 3-pin screw clamp (Fig ii). The PEGDA and photo-initiator solutions were injected and UV cross-linked for 10 min. After the hydrogel was cured, the shear stress before the point of adhesive failure was recorded by TCD110 Series Force Measurement System (Chatillon Force Measurement Products, USA) with a maximum load of 10N while moving upwards at a controlled strain rate of 5 mm/min. The value recorded was the maximum force required for the complete detachment of hydrogel from the surface and this value was then divided by the interfacial area contacting the hydrogel and stent surface, denoted by $\pi \times 0.167\ \text{cm} \times 2\ \text{cm} = 1.05 \times 10^{-4}\ \text{m}^2$ in order to derive the force of adhesion per unit area between the hydrogel and stent interface in N/m^2. 5 sets of measurements were done for each parameter (n = 5).

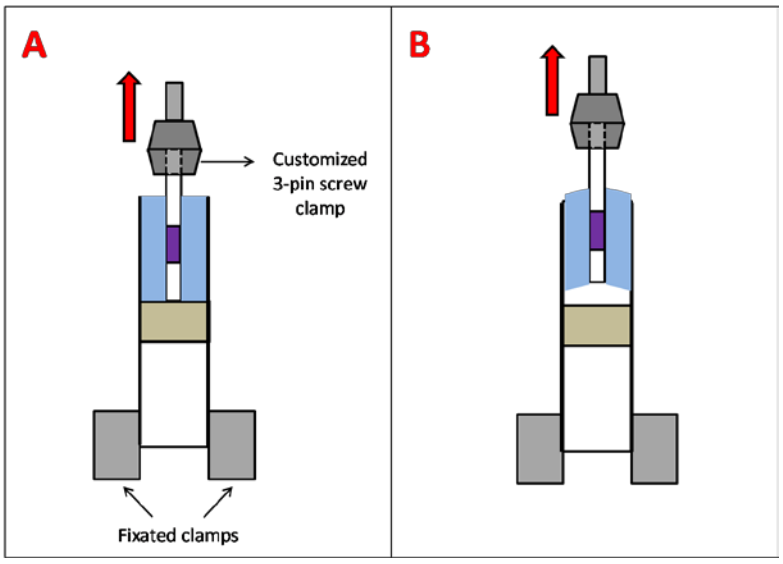

Fig ii. ***Schematic diagram for the experimental set-up of shear adhesion delamination test.***(A) Before pull-off begins, (B) After pull-off completes

2.4 In vitro drug release study

2.4.1 Effect of polymer thickness and drug loading on drug release under static condition

The samples listed in Table 1, (in each group, n = 3) were immersed in a vial containing 5 mL PBS (pH = 7.4) and incubated at 37^{o}C throughout the release study. At each predetermined time point over a 4-week study, 1 mL of the release medium was drawn and its mitomycin C concentration was measured with reversed-phase High Performance Liquid Chromatography (HPLC, Agilent 1100). The release medium was then replaced with fresh 5 mL volume of PBS (pH = 7.4) and the measurement was repeated at subsequent time points. Concentrations of mitomycin C were measured at 365 nm using a ZORBAX Eclipse XDB-C18 column (250 mm × 4.6 mm, pore size of 5 µm). The isocratic mobile phase consisted of 75% (v/v) water, 25% (v/v) methanol, 0.5% (v/v) acetic acid and 0.02 M ammonium acetate, with a flow rate of 1 mL/min. Mitomycin C retention time is about 11 - 12 min. The cumulative drug release (in % and µg) was calculated and plotted ***(Refer to Supplementary Section, Part III)***.

Table 1

Effect of polymer thickness and drug loading on drug release (static)

Sample name	MMC loading (% w/w)	Thickness of coating (µm)	Amount of MMC loaded (µg)
A	5	50	360 ±20
B	5	120	990 ± 10
C	5	240	2000 ± 30
D	2.5	50	150 ± 5
E	5	50	400± 20
F	7.5	50	560 ± 60

2.4.2 Effect of PEGDA hydrogel on the in-vitro drug release and ex-vivo drug transfer under static and dynamic fluid flow conditions

The samples listed in Table 2 were assessed under two different conditions. Firstly, the effect of PEGDA hydrogels on drug release was assessed in a static condition over 4 weeks [using HPLC (Samples G - H) to quantify drug] and in a dynamic fluid flow condition for 1 week [using Liquid chromatography mass spectroscopy (LCMS) (Samples I - J) to quantify drug]. The dynamic fluid flow experiment was set up using a

customized glass apparatus design to mimic an adult human physiological urinary system at physiological urine flow rate of 0.5 mL/min (Fig iii)[33, 34]***(Refer to Supplementary Section, Part IV)***.

Next, the *ex-vivo* drug transfer was evaluated under dynamic fluid flow conditions through an explanted porcine ureter, over 2 days (Samples K - L). At the end of experiment, the ureter was removed and drugs extracted using solid phase extraction (SPE) techniques and then quantified using LCMS.

The SPE method was performed as follows: 1 mL SPE tube, Strata^{TM}–X, 33 µm polymeric reversed phase (surface modified styrene divinylbenzene), polymeric sorbent mass = 30 mg/mL (Phenomenex), was used. The SPE tubes were first connected to a vacuum manifold which allowed for controlled solvent flow rate. Next, the tubes were conditioned using methanol (2 mL), followed by ultrapure water (2 mL). After that, 1 mL of the samples were added to the packing and allowed to elute slowly (< 1mL/min). A series of washing steps were performed in the order: Water (1 mL) × 2, 90% water/10% methanol (1 mL) × 1, and 70% water/30% methanol (0.2 mL) × 1. The samples were then allowed to dry with nitrogen for 5 min. Finally, the analyte retained on the packing was eluted twice using 70% water/30% acetonitrile (0.5 mL × 2) at a controlled flow rate (<1 mL/min). The drug extracted was filtered using 0.22 um membrane filter (Durapore) and then quantified using LCMS (Waters).

The LCMS method was as follows: For the LC method, Acquity UPLC H Class (Waters) and Acquity UPLC BEH C18 column (50 mm× 2.1 mm × 1.7 um) (Waters) were used and column temperature set to 40^{o}C. The mobile phase comprised isocratic elution of 90% water and 10% acetonitrile with 0.1% (v/v) acetic acid, at a flow rate of 0.2 mL/min for run time of 5 min. For the MS method, Acquity Xevo TQ-S Micro MS detector (Waters) was used. The electrospray was operated in the positive ionization mode (ESI+) and the MMC and IS were identified in the multiple reaction monitoring (MRM) mode. The following tuning parameters were employed: Capillary voltage (2.80 kV), desolvation temperature (450^{o}C), desolvation gas flow (800 L/h), cone gas flow (70 L/h) and source temperature (150^{o}C). The parent $[MMC+H]^{+}$ ion generated two daughter ions at m/z 214.756 (cone voltage = 6V, collision energy = 28V) and m/z 242.064 (cone voltage = 6V, collision energy = 8V), while the parent $[PFM+H]^{+}$ ion generated two daughter ions at m/z 241.032 (cone voltage = 8V, collision energy = 26V) and m/z 256.057 (cone voltage = 8V, collision energy = 10V). The monitoring ions of MMC and PFM were m/z 242.064 and m/z 256.057, respectively, which were used for the quantification of drug in the tissue samples.

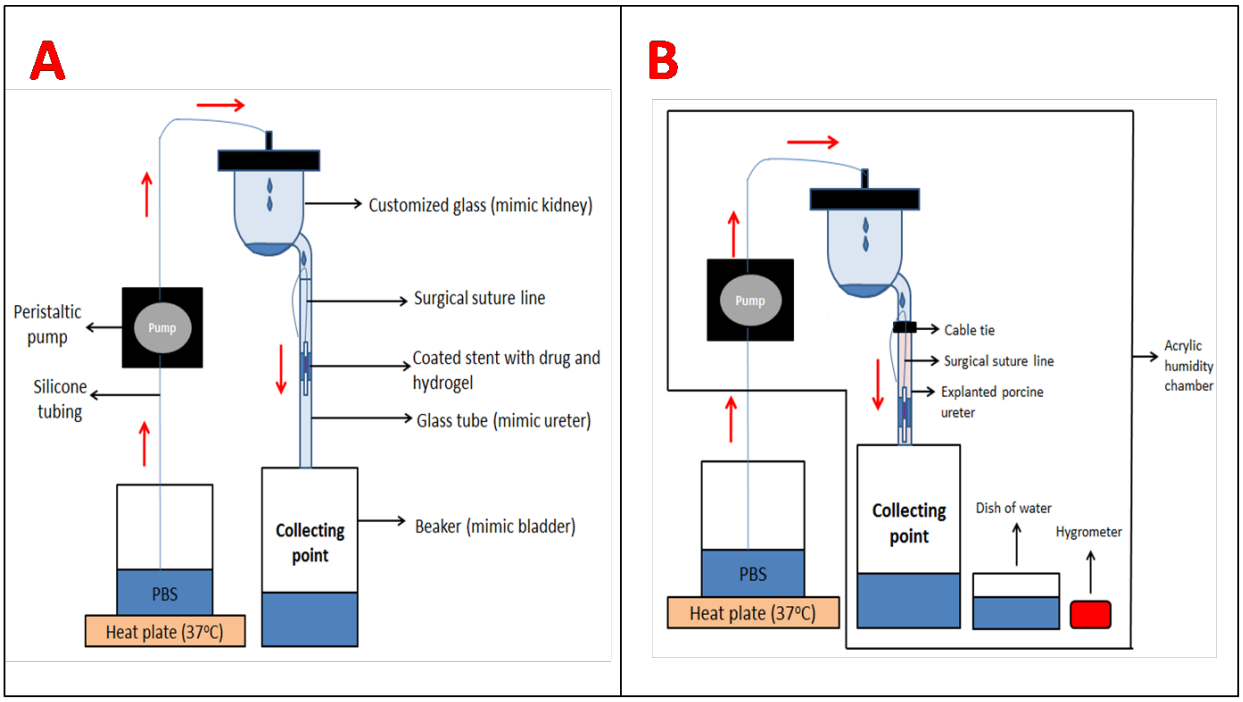

Fig iii. ***Schematic diagram for the dynamic fluid flow model***.(A) For drug release study, (B) For drug transport study

Table 2

Effect of PEGDA hydrogel on drug release (static and dynamic) and drug transfer

Sample name	MMC loading (% w/w)	Thickness of coating (μm)	PEGDA (% w/v)	Amount of MMC loaded (μg)
G	5	50	-	360 ± 30
H	5	50	10	340 ± 30
I	5	50	-	180 ± 10
J	5	50	10	160 ± 10
K	5	50	-	200 ± 20
L	5	50	10	160 ± 20

2.5 Effect of drug released from bilayer coated stents on cell proliferation

HBdSF cells were seeded into 24-wells plate with approximately 2 mL (~12,000) cells in each well. Cells in passage 7 were used in the experiment. The cells were allowed twenty-four hours for attachment onto the walls of the wells before the experiment began. All the fabricated stents were first sterilized using ethylene oxide gas and then

placed in the well using a permeable Transwell® cell culture insert (8 µm pore size) (Falcon, USA), so that the stents were not in direct contact with the seeded cells. 2 mL of 0.5 µg/mL of mitomycin C was also added as a control to investigate the effect of the drug-eluting stent on the cells. Following incubation at 37^{o}C / 5% CO_2 for 3 days, the cell culture media was removed and the wells were rinsed with 1x DPBS thrice. To study cell proliferation behavior, Prestoblue® cell viability reagent was used. 900 µL cell culture medium was pipetted into each well and then 100 µL of Prestoblue® reagent was added. The plate was re-incubated for 30 min under 37^{o}C / 5% CO_2. Subsequently, 70 µL of the culture medium/viability reagent was transferred to a black microplate for analysis. Table 3 lists the test conditions (in each group, n = 3). All assays were read using a multi-well plate reader (Tecan, Infinite® 200) using fluorescence excitation wavelength of 560 nm and emission wavelength of 590 nm.

Table 3

Transwell migration experiment

Sample name	Presence of stent	MMC loading	Durations of plasma treatments (min)	Duration of UV irradiation (min)	PEGDA (% w/v)	Irgacure-2959 (% w/v)
M	No	-	-	-	-	-
N	No	0.5 µg/mL	-	-	-	-
O	Yes	-	5	10	10	0.1
P	Yes	5% w/w (360 ±20µg)	5	10	10	0.1

2.6 In-vivo feasibility study

A study aimed at evaluating the feasibility of the device prototype to swell and deliver drugs to the urothelium was conducted on 1 adult female pig weighing 34 kg (*Sus scrofa,* bred at National Large Animal Research Facility (NLARF) for research and training purposes in Singapore) in adherence with National Advisory Committee on Laboratory Animal Research (NACLAR) guidelines, with approval from Institutional Animal Care and Use Committee (2016/SHS/1237). The animal study was carried out at SingHealth Experimental Medicine Centre (SEMC) on Singapore General Hospital (SGH) Academia campus.

The purpose of this study was to evaluate the feasibility of the device prototype to swell in ureter to co-apt with the urothelium in order to deliver drugs locally to the targeted site, mainly the middle ureter section *in-vivo*. This was a proof of concept feasibility study in a porcine model using one animal. The porcine model was selected due to the

physiological resemblance of porcine ureter with human ureter in terms of physiology and physical dimensions[35]. The animal was anesthetized using TKX cocktail (0.05 mL/kg, IM) and atropine sulphate (50µg/kg, IM). Before the implantation, the animal was administered with analgesics (Tramadol, 2-4 mg/kg, IM) and antibiotics (Synulox, 0.05 mL/kg, IM) once. Intra-operatively, the anesthesia was maintained using 1-3% Isoflurane. Electrocardiogram (ECG), respiration rate, heart rate and oxygen saturation were also monitored and recorded during the operation.

A bilayer coated stent (with base ureteric stent of outer diameter 6 Fr and 24 cm in length) was fabricated in the laboratory and was implanted into the right ureter while a bare stent (6 Fr) of the same length was implanted in the contralateral ureter as control. The test stent was coated with 7.5% w/w MMC over 3 cm in the middle (400 µg) pre-treated with plasma (100W, 5 min) and then a layer of 10% w/v PEGDA hydrogel was coated over 9 cm of its middle section with the use of a plastic mold tubing with 6 mm internal diameter. Both stents were sterilized with ethylene oxide (ETO) before use. It has been reported that the mechanical performance of PEGDA hydrogels was unaffected by ETO sterilization process[36]. To facilitate stent insertion and maneuverability, the hydrogel layer was designed to comprise 2 tapered ends. The outer diameter of the coated section in the dry state was around 2.8 mm and can swell to approximately 7 mm when fully swollen after 1 day immersion in phosphate buffered saline (PBS).

An intravenous urogram (IVU) was carried out to image the urinary tract by injecting 100 mL of Omnipaque contrast (300 mg I/ mL) via the auricular ear vein. This was followed by cystoscopy and identification of the ureteric orifice. The Seldinger technique for stent insertion was employed over a guidewire. Before device implantation, the coated stent was immersed in Omnipaque^{TM} contrast (300 mg I/ mL) for 2 min and then briefly in normal saline to promote X-ray visualization and to offer lubricity for ease of stent placement, respectively. The stent placement was performed via the retrograde method, in which a hydrophilic guidewire (Terumo, Radiofocus® Guidewire M angled 0.035^{o}) was first inserted into the tract using a cytoscope (Karl Storz) and the device prototype railroaded through the wire before being implanted into position with the aid of a pusher. The wire was withdrawn thereafter and device then left in animal for a day. Twenty four hours after stent insertion, another IVU was performed to ascertain whether the hydrogel had achieved close apposition with the urothelium. Euthanasia using pentobarbital sodium (300 mg/mL) via intravenous route was then performed. Following this, a laparotomy was performed by diathermy (Valleylab, Force FX) to expose the bilateral ureters before the latter were harvested and divided into 3 segments, comprising of proximal, middle and distal sections, each of 6 cm in length.

The tissue samples were analyzed for presence and quantity of MMC using LCMS. Blood (10 mL) and serum (10 mL) were also collected into EDTA tubes before the

device implantation on day 0 and after animal sacrifice on day 1. These were analyzed to evaluate any signs of systemic toxicity and kidney damage. Tissue and blood analysis were performed using SPE and LCMS ***(Refer to Supplementary Section, Part V)***. Serum creatinine levels were assessed using spectrophotometry.

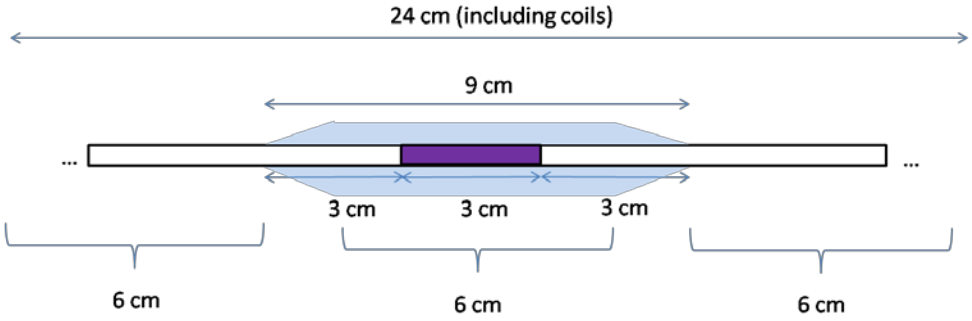

Fig iv. ***Schematic diagram for the coated stent prototype in in-vivo feasibility experiment***

2.7 Statistical analysis

All studies were performed with a minimum of triplicates (except for XPS analysis) and statistical significance was determined by two-tailed unpaired Student's t-test. Differences were considered significant at *p< 0.05. Data was expressed as mean ± standard deviation (SD).

3. Results

3.1 Evaluation of PEGDA hydrogels

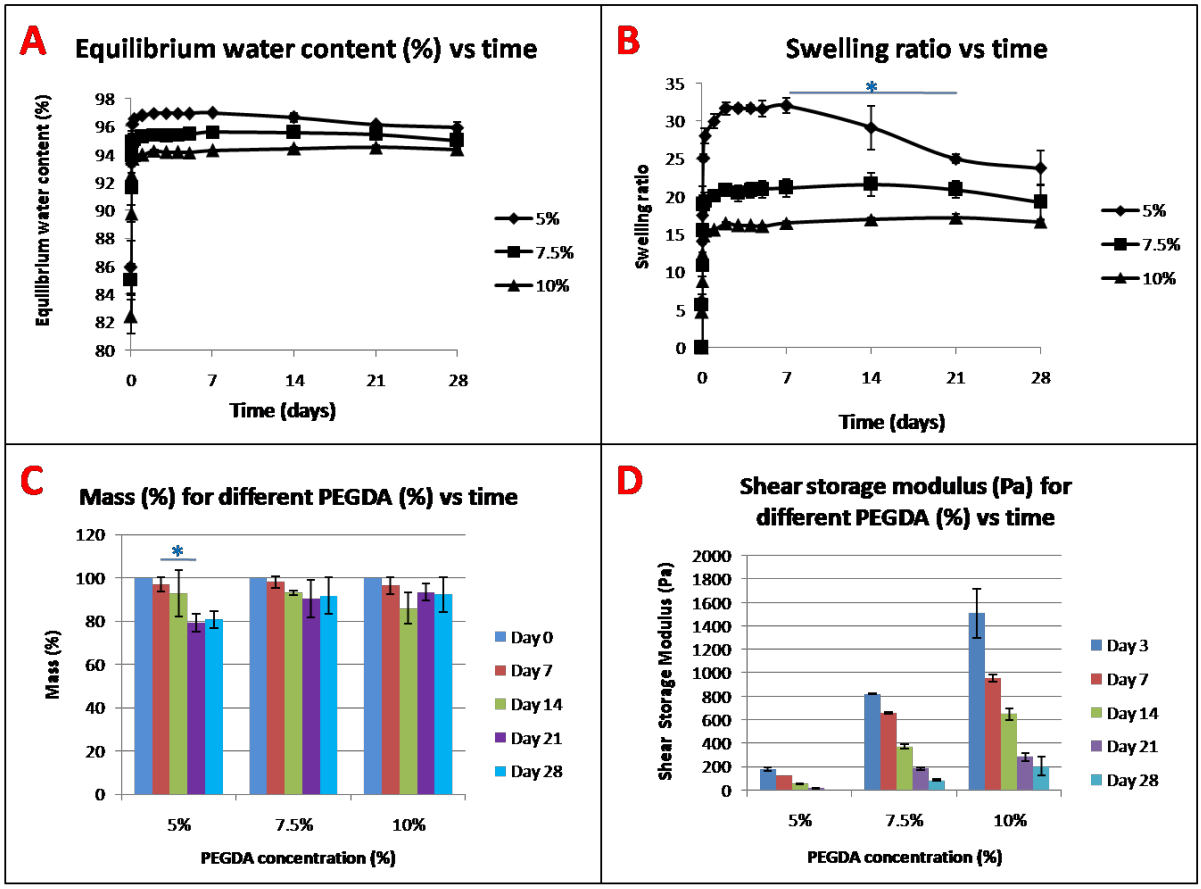

Fig 1.***Characterizations of PEGDA hydrogels***.(A) Equilibrium water content (%), (B) Swelling ratio, (C) Mass loss (%), (D) Shear storage modulus (Pa)

PEGDA hydrogels attained equilibrium swelling by Day 3 with high equilibrium water content above 90%up to 28days (Fig 1A). The swelling ratio of the PEGDA hydrogels correlated inversely with their PEGDA concentrations: 30 times for 5% > 20 times for 7.5% > 15 times for 10% w/v PEGDA. Swelling ratio for 5% w/v PEGDA hydrogel showed significant reduction from Day 21 onwards (*$p < 0.05$), while no significant changes were observed in the other two groups (Fig 1B). Although no significant mass losses over 28 days was recorded for 7.5% and 10% w/v PEGDA hydrogels (Fig 1C), their shear storage modulus gradually decreased over the same time period (Fig 1D). In contrast, 5% w/v PEGDA lost significant mass from 97% on Day 7 to 79% on Day 21 (*$p < 0.05$).

3.2 Evaluation of surface plasma treatment

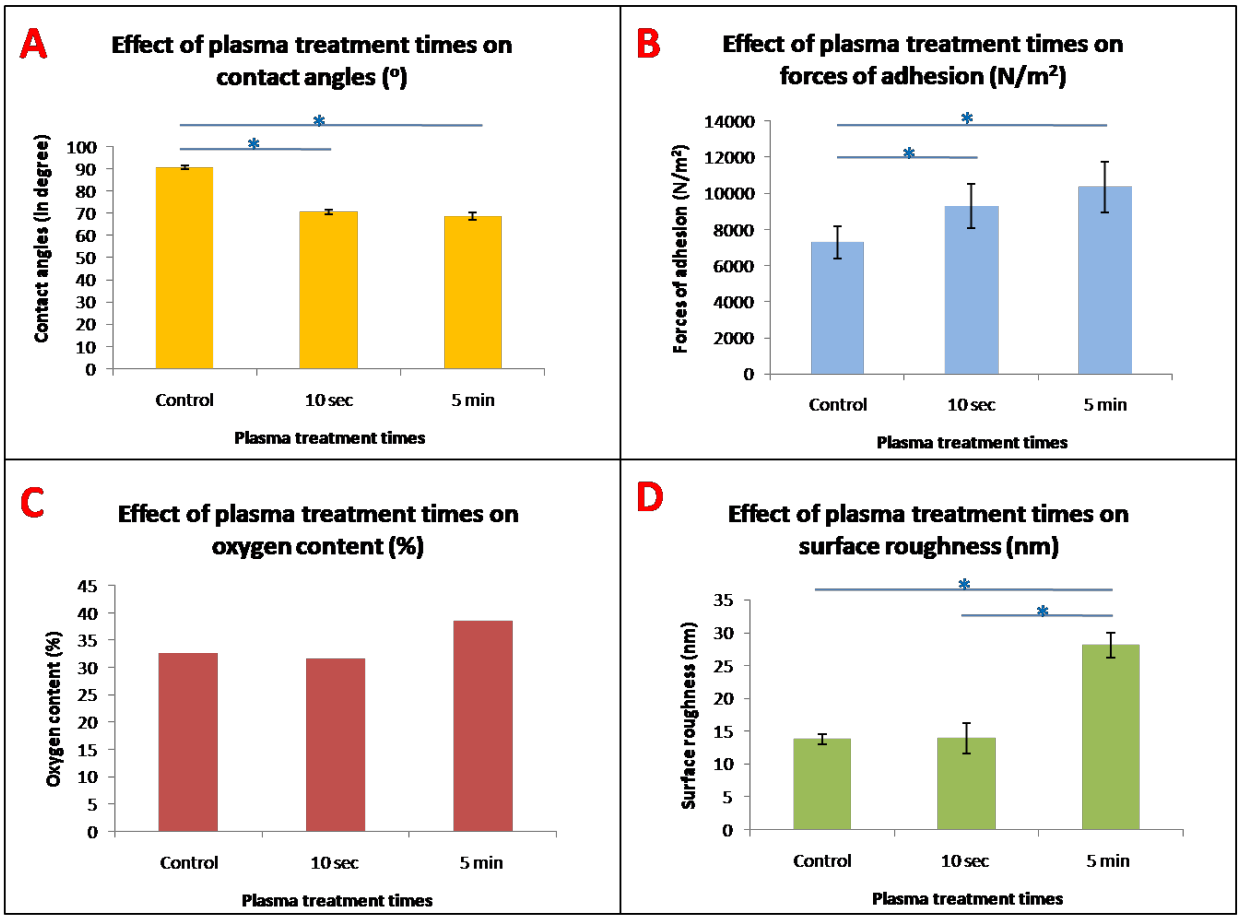

Fig 2.***Characterization of plasma surface treatment***.(A) Contact angles, (B) Surface roughness (AFM),(C) Surface oxidation (XPS), (D) Shear adhesion delamination forces.

As good interfacial adhesion between the PEGDA hydrogel and stent is required to withstand shear forces encountered during stent deployment (i.e. stent insertion and removal), oxygen plasma treatment was conducted on the PLC-coated stents to improve PEGDA hydrogel adhesion to the PLC layer. Plasma treatment times of 10 s yielded a significant reduction of contact angle measurements from 91 ± 1^{o} to 71 ± 1^{o} (*$p < 0.05$), however, no marked reduction in contact angle was observed when plasma time was prolonged to 5 min (70 ± 2^{o}) (Fig 2A). AFM demonstrated that a longer duration at 5 min induced a significantly rougher surface (28 ± 2 nm) compared to both 10 s treatment (14 ± 2 nm) and control (14 ± 1 nm) (*$p < 0.05$) (Fig 2B). This is corroborated by XPS data, with a nominal penetration depth of 0-9 nm, which indicates enhanced oxygen content at longer plasma duration (Fig 2C). The plasma treatment duration alters the structure of the surface region, potentially impacting its durability, following deployment. A shear adhesion delamination test demonstrated that the forces required to detach the hydrogel from the PLC-coated stent was increased upon plasma treatment from 7300 ± 900 N/m^2 (control) to 9300 ± 1200 N/m^2 (10 s plasma) and 10400 ± 1400 N/m^2 (5

min plasma) (*p < 0.05), whereas 10 s and 5 min plasma treatment times did not show any significant differences in the forces required (Fig 2D).

3.3 Evaluation of the effect of polymer thickness and drug loading on drug release under static condition

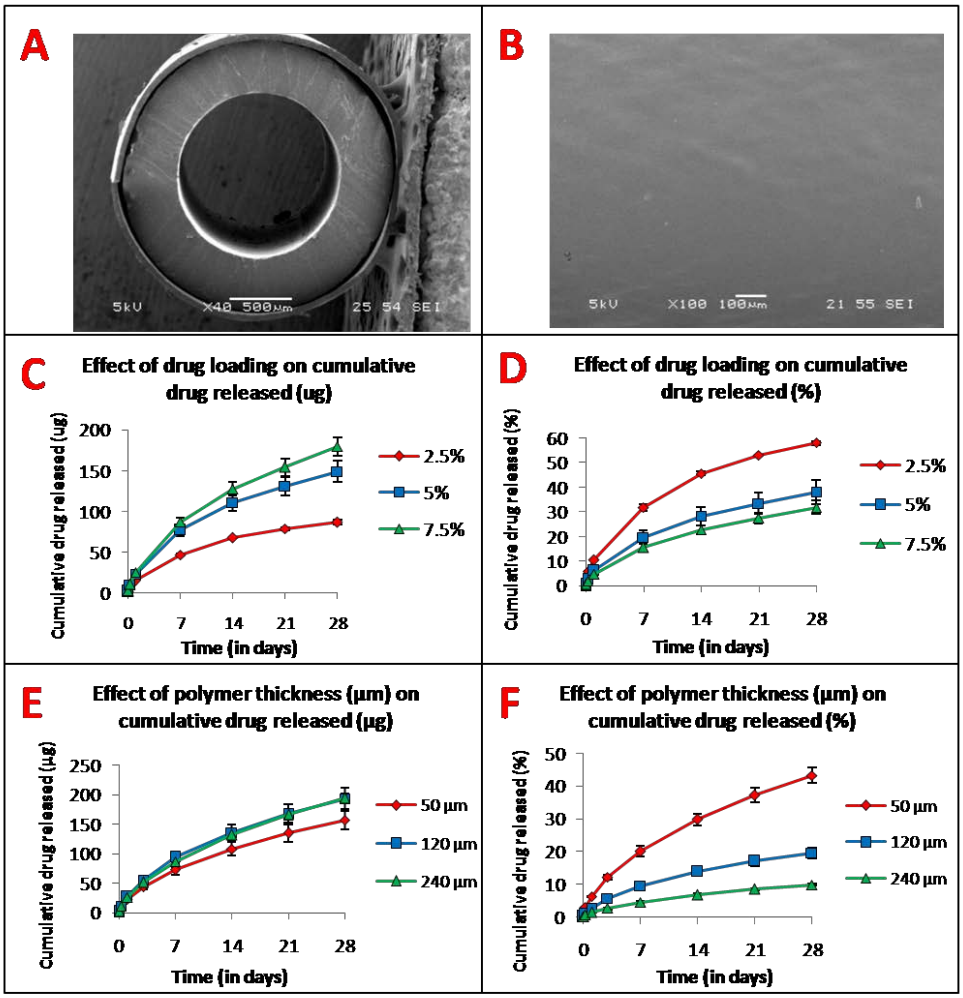

Fig 3.***Drug release studies in static condition***.(A) SEM image of cross-section, (B) SEM image of surface morphology, (C) Effect of polymer thickness on drug release (µg), (D) Effect of polymer thickness on drug release (%), (E) Effect of drug loading on drug release (µg), (F) Effect of drug loading on drug release (%)

The drug coating was successfully applied to the stent (Fig 3A), resulting in a smooth surface morphology (Fig 3B). Decreasing the drug loading and the polymer thickness led to faster drug release rates (Fig 3C-3F). The drugs were sustainably released over the 28 days and will likely continue beyond the 1 month period.

3.4 *Evaluation of the effect of PEGDA hydrogel on the in-vitro drug release and ex-vivo drug transfer under static and dynamic fluid flow conditions*

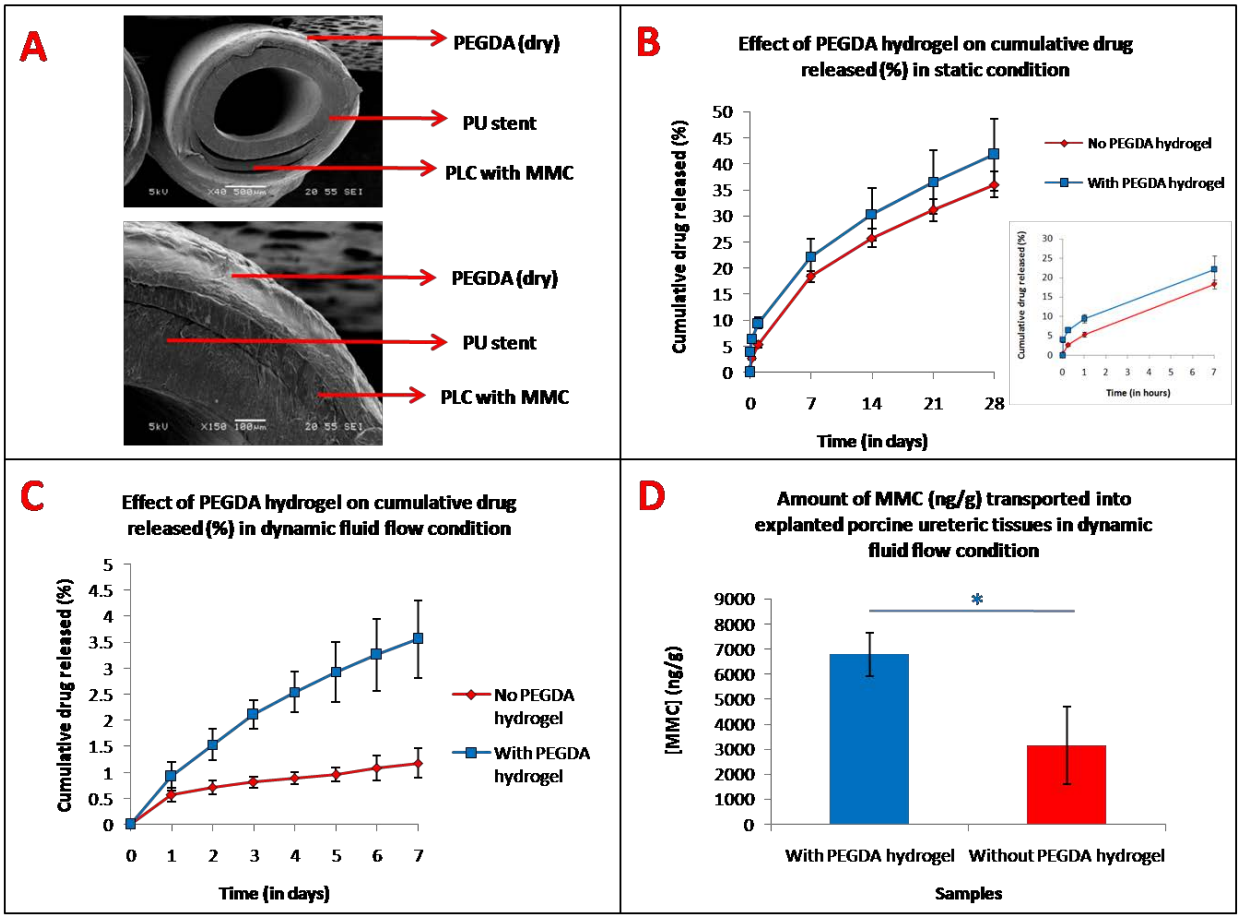

Fig 4.*Effect of PEGDA hydrogel on drug release and drug transport.*(A) SEM image of the cross-section of bilayer coated stent, (B) Drug release in static condition, (C) Drug release in dynamic fluid flow condition, (D) *Ex-vivo* drug transport in dynamic fluid flow condition

PEGDA hydrogel was coated over the first drug layer (Fig 4A) and did not delaminate from the stent after its immersion in phosphate buffered saline at 37^{o}C for the 4-weeks period. In static conditions, the hydrogel did not significantly alter drug release rates, except during the first-hour time point (Fig 4B). However, under dynamic fluid flow, a markedly greater amount of drugs (around 3 times greater on Day 7) was released *in-vitro* (Fig 4C) and transported into the explanted porcine ureteric tissues *ex-vivo* (Fig 4D) with 7 $\pm$1 ng/g MMC detected, compared to 3$\pm$2 ng/g when hydrogel was absent (*p

<0.05). The greater drug release due to PEGDA hydrogel is advantageous to mediating as much drug transfer to the tissues as possible.

3.5 Evaluation of coated stents on HBdSF

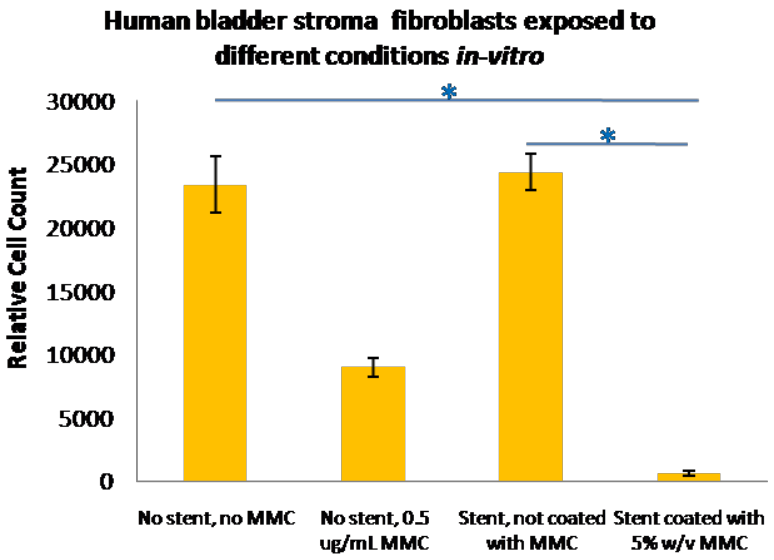

Fig 5.Cell assay study

Segments of stents, coated with PLC and PEGDA hydrogels, were placed on individual permeable Transwell® membrane inserts, to allow eluted MMC to reach HBdSF cells cultured in the lower compartment. HBdSF cell growth, at 3 days, in the presence of PLC and PEGDA (crosslinked with 0.1% w/v photo-initiator) but without MMC, was similar to the untreated control. The elution of MMC from the coated device induced a sharp decrease in HBdSF, over the 3-days' culture, as compared to having no stent and a stent coated with only PLC and PEGDA hydrogel, due to the higher MMC concentrations ($p^* < 0.05$) (Fig 5).

3.6 Evaluation of feasibility and safety of coated stent prototype in-vivo

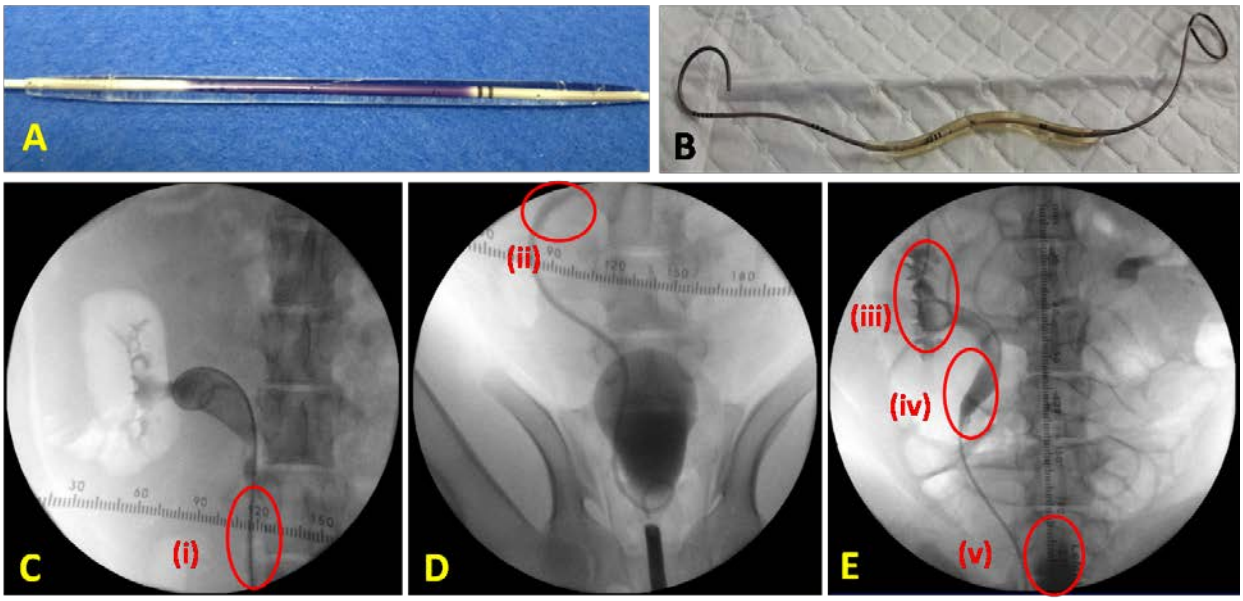

Fig 6.***Pilot in-vivo study: Images.*** (a) Bilayer coated stent, (b) Coated stent removed after the study, (c, d) IVU taken on Day 0 upon coated stent insertion, (e) IVU taken on Day 1 just before coated stent removal

A coated stent prototype was successfully fabricated and evaluated in a single pig, assessing its deployment feasibility and the configuration for drug transfer, in contact with the urothelium at the middle ureteric section (3 - 4 mm in inner diameter) where the hydrogel coating is expected to co-apt but not substantially adhere to (Fig 6A). The coated stent could be inserted into the ureters without undue resistance. Due to the immersion into Omnipaque^{TM} prior to stenting, the hydrogel section was observable under X-ray (Fig 6C and 6D). After 1 day, IVU images showed the radio-opaque agent accumulated in the region adjacent to the hydrogel section of the stent, thus indicating an apposition of the hydrogel coating with the ureteric wall and no observable stent migration (Fig 6E, iv). The apposition was believed to be substantial in this study since the hydrogel coating section has been designed to swell up to around 7 mm outer diameter, much higher than the diameter of the middle ureteric segment where the hydrogel was targeted to co-apt with. In addition, it was subsequently observed that the contrast agent flowed within the stent's hollow lumen, into the bladder (Fig 6E, v). After animal sacrifice, both harvested ureters showed that the hydrogel layer remained adhered to the device with no delamination and the outer diameter of the coated section measured at approximately 7 mm (Fig 6B). Moreover, observation of the kidney calyx indicated that there was no distension or swelling (Fig 6E, iii).

A

Sections analyzed	Absolute amount of MMC (ng)	Total mass of tissue samples analyzed (g)	Amount of MMC per gram of tissues (ng/g)
Proximal (Test)	4.1	1.6	2.6 ± 1.2
Middle (Test)	384	1.9	202 ± 92
Distal (Test)	4.4	1.8	2.5 ± 1.5
Peri-ureteric fats (Test)	3.6	0.3	15 ± 30

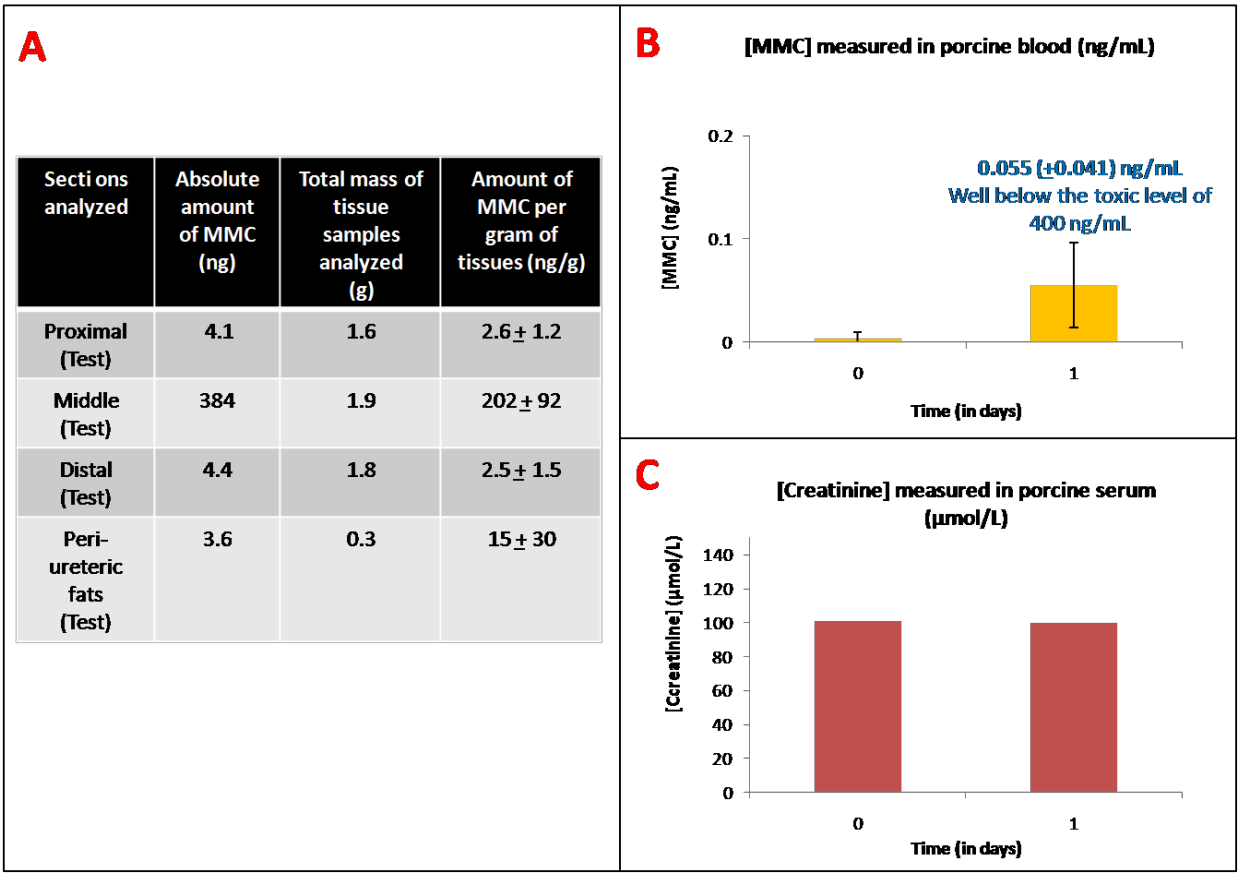

Fig 7.***Pilot in-vivo study: Results*** (A) Amount of MMC in porcine ureteric tissues, (B) Amount of MMC in porcine blood, (C) Amount of creatinine in porcine serum

A significant amount of MMC was found in the central segment of the stented ureter (at close to 400 ng) where the targeted coated section co-apted with the urothelium as compared to other segments, either where no stent was implanted or when no drugs were coated onto the stent sections (Fig 7A).There was also negligible level of MMC in the peri-ureteric fat segment (Fig 7A) and in porcine blood (Fig 7B), following one day implantation. Analysis of the creatinine level before and after the in-vivo study, showed that it remained stable at around 100 µmol/L (Fig 7C).

4. Discussion

A novel bilayer coated ureteric stent prototype has been successfully prepared and assessed, for its feasibility to swell and co-apt with the urothelium, in order to transfer drugs locally to targeted ureteric site. Different outer diameters of the hydrogel coating can be made by customizing varying diameters of the plastic mold tubing. Herein, a 6-mm diameter tubing was used to fabricate a coated stent device that swells up to a maximum of around 7 mm; No further expansion of the hydrogel section on the stent was recorded beyond this dimension mark following continuous immersion of the device

in phosphate buffered saline since the hydrogel has attained equilibrium swelling without significant changes in the swelling ratio and water content. The ureteric diameters may vary along the length (proximal, middle and distal sections) [37], however, the swollen hydrogel coated in the selected stent region has been designed to be always wider (10 - 20%) than that of the targeted ureteric segment so that a close apposition of the hydrogel with the urothelium is expected to be achieved. 7.5 - 10% w/v PEGDA hydrogel presented swelling ratios of 15 - 20 times and maintained mechanical stability without significant mass loss over 4 weeks. Plasma treatment (5 min, 100W) prevented hydrogel delamination from the drug coating in the 4-weeks study *in-vitro* in static condition. PEGDA hydrogel significantly enhanced drug release and drug transfer into the explanted porcine urothelium, under dynamic fluid flow conditions. The mechanical and functional validation of the device to be deployed and removed, as well as to swell and to contact with the urothelium to transfer drugs to the urothelium, was also successfully demonstrated in one porcine over one day indwelling duration in the pilot *in-vivo* proof-of-concept study.

The high hydrogel water content (>90%) is expected to enable the hydrophilic drug MMC to partition readily and thus be delivered to the target ureteric tissue. The reduction of the swelling ratio with increasing PEGDA concentration putatively resulted from the increase in crosslink density, which hindered polymer chain expansion [38]. The marked decrease in swelling ratio from Day 7 to 21 for 5% w/v PEGDA could be attributed to the onset of its degradation. This is corroborated by a corresponding mass loss, which could be due to the hydrolytic breakdown at crosslink and leaching of PEGDA chains. Interestingly, the decrease in storage modulus with time, for 7.5% and 10% w/v PEGDA concentrations, can be attributed to the crosslinking breaking down, but not sufficient enough to allow PEGDA to leach out of the bulk. Since 10% w/v PEGDA experienced no significant mass loss over the 28 days and possessed the highest shear storage modulus, it is expected to withstand mechanical manipulation most effectively in clinical applications.

Contact angle and atomic force microscopy measurements demonstrated the importance of surface plasma treatment of the drug coating to increase surface wettability and roughness, which are essential prerequisites for the enhancement of interfacial adhesion. A 10-second exposure decreased water contact angles, however no observable improvement was recorded when exposure time was increased to 5 min. This could be due to the saturation of oxygen groups on the treated surface, as reported by R. Landgraf *et al*. in which 30 s of 100W plasma treatment could saturate oxygen content on epoxy-based polymers[39]. A significant increase in surface roughness, on the other hand, was recorded only with longer plasma exposure of 5 min. It has been well documented that prolonged plasma etching induces surface roughness[40].The shear adhesion delamination test showed similar improvement, in the forces required

for hydrogel detachment for both 10 s and 5 min plasma exposure. Nevertheless, 5 min plasma time was chosen as the preliminary plasma duration for this study. The importance of the adhesion testing on stent coatings was exemplified in another study that measured the binding between poly(lactide)(PLA) and poly(p-xylylene)(PPX)-coated metal cardiovascular stent[41]. Several studies have also reported about imparting surface roughness for the augmentation of the interfacial work of adhesion between adjoining surfaces[42, 43].

Sustained drug release is therapeutically relevant for the treatment of chronic conditions, as it provides for long term dosing with a single treatment[6]. The drug release (%) rates decreased as expected, with an increase in drug loading; this is true when the amount of drug loaded (C_o) is greater than the saturated amount of drugs (C_s) in the polymer matrix[44]. On the other hand, a thicker polymer coating released the drug at a slower rate, due to its longer diffusion path length[45]. This implies that the drug release can be tuned with these parameters. Furthermore, there was no significant burst release of drugs, with only about 7-9% of the loaded drug released within the first day. Moreover, no bulk or surface erosion was likely to have occurred as the surface topography remained smooth, following the 28 days study. This is reasonable, given that PLC requires more than a month for the onset of degradation[46]. The drug release from the PLC coating (a matrix-type system) during the 4 weeks period is thus ascribed to Fickian diffusion[47]. The daily released drug dosage was calculated to be above the minimum effective concentration of MMC, for inhibiting human bladder stroma fibroblasts over 3 days of incubation *in-vitro* (0.01 µg/mL) ***(Refer to Supplementary Section, Part VI)***.

In the static condition, drug release from the stent coated with PEGDA hydrogel did not significantly alter the drug release rate, as compared to the coated stent in PBS, except for during the first hour. This could be due to the similar manner in which the hydrogel mimicked an aqueous solution with high water content (>90%). An initial higher drug release could be due to a small amount of drug partitioning into the hydrogel phase from the PLC phase, prior to the stent being exposed to PBS medium. In addition, the plasma treatment (100W, 5 min) promoted the attachment of hydrogel over the 4-weeks period in the static medium of PBS at 37^{o}C, without altering the drug release amount, since the bulk properties remained intact with the plasma treatment[48].

Under the simulated urodynamic fluid flow conditions, at physiological urine flow rate of 0.5mL/min, drug release was generally slower than observed in the static conditions, regardless of the presence or absence of the hydrogel coating. This can be attributed to a shorter contact time of the dynamic fluid with the drug/gel coatings. An increased drug release in the presence of PEGDA hydrogel in the dynamic condition is likely due to the polymer/drug layer in contact with a larger amount of water content in the hydrogel. This is consistent with a finding by Pimenta *et al.,* who compared diclofenac release from

hydroxyethyl methacrylate-based hydrogel[49], where 90% diclofenac release was attained by 100 hours in dynamic flow, as compared to 24 hours in static condition. Although other groups have drawn similar comparisons between static and dynamic conditions in the other application models [50-52], our study is the first to compare drug release in static and dynamic condition in an urodynamic condition.

More significantly, it was also found that more drugs were delivered to the porcine ureteric tissues *ex-vivo* from a stent coated with PEGDA hydrogel. This can be explained by an increased amount of drug released, as well as the close apposition of the hydrogel with the ureteric tissues in the current study. PEG-based hydrogel is a well-suited material, given that PEG was reported to have enhanced bioadhesion to urothelial mucosa[53].

Cell cyto-toxicity experiments demonstrated that MMC remained active in reducing the fibroblast cell lines, even after the stents have been subjected to plasma modification (100W, 5 min) and ultraviolet irradiation (365 nm, 10 min). Moreover, the studies also demonstrated polyurethane, PLC and PEGDA materials to be cyto-compatible *in-vitro*. 0.1% w/v Irgacure 2959 photo-initiator was also not cyto-toxic to the cells *in-vitro*. These confirm the feasibility of using 5 min plasma treatment time *in-vitro*, since drug activity and release remain unaffected by the fabrication process. Furthermore, more cell death was recorded for the coated stent samples than for the media control (0.5 µg/mL MMC solution). This was due to the higher MMC amounts released from the stent sample. Referring to Fig 3C, there was an estimated 8 µg/mL MMC cumulatively released over 3 days in the 5 mL phosphate buffered saline (PBS), which was much greater than 0.5 µg/mL.

The coated stent was successfully implanted and removed in the porcine ureter using the current standard protocol for stent insertion in patients. Since both the urothelial lining and hydrogels were hydrophilic and lubricious, there was no significant friction that resisted the movement of stent along the tissues [54]. The radio-opacity of the hydrogel, generated by its exposure to Omnipaque^{TM} solution, enabled the clinician to visually locate the coated section of the device under fluoroscopic guidance. Although bilayer coatings were applied to the central section of the stent, these could similarly be applied onto other selected sections (upper/distal) of the stent. The flow of contrast fluid around the stent was restricted, as indicated in the X-ray image, due to an apposition of the external hydrogel coating with the ureteric wall. Antegrade flow of contrast agent within the stent lumen was unimpeded as there was no evidence of obstruction of dilation of the proximal kidney. This could explain why no urine backflow (hydronephrosis) is believed to have occurred, given that the kidney calyx maintained its healthy original shape and size.

The feasibility of this device, to locally deliver drugs in a targeted fashion within the ureter, was demonstrated by drug detection in only the central section of the stented ureter and nowhere else along the harvested urothelium. However, the drug quantity was significantly lower than that transported to urothelium *ex-vivo*. This may be caused by the abolishment of the peristaltic movement of the ureter *in-vivo*, rendering drug transfer more challenging due to the ureteric dilatation[33, 55]. Furthermore, it is important to note that 400 ng/mL MMC in porcine blood is considered as toxic to the animal[56] and an abnormally large increase in serum creatinine implies that kidney might be damaged[57]. In our study, negligible amount of drug was detected in the peri-ureteric fats, serum creatinine and blood, demonstrating the absence of systemic toxicity and kidney damage.

5. Conclusion

This is the first demonstration of a swellable drug-eluting ureteric stent both *in-vitro* and in preliminary pilot *in-vivo* proof-of-concept study. The mechanical and functional validation of the device to achieve apposition with the urothelium upon swelling, as well as its performance in delivering drugs to the targeted ureteric region, over 1 day of indwelling stent duration in one porcine without significant systemic levels, have been observed. The ease of inserting and removing the stent in the porcine model with current clinical practice has also been demonstrated *in-vivo*.

The hydrogel-expandable drug-eluting polymer coating may potentially be applied to other areas in the urinary tract including urinary catheters used in the lower tract for treatment of strictures. The coating may also be applied onto other stents in body lumens for disease management, such as in the esophagus and colon.

6. Limitations

Longer-term studies with a larger sample size in an *in-vivo* setting are desired for a more comprehensive evaluation of the prototype, in terms of establishing the device safety, therapeutically relevant amount of drug for the efficacious treatment of the particular urologic disease such as carcinoma and the range of safe drug dosage. Future work will also investigate the distribution of the drugs in the urothelium, as it has been widely reported that the drug should reach the smooth muscle cells layer to exert pharmacological effect in the case of stricture management [26, 58]. A study to investigate the effects of ureteric flexing and bending due to the pigs' mobility is also crucial for the validation of the hydrogel durability during stent indwelling duration. The presence of any possible iatrogenic injury to the ureters due to device removal could also be observed by examining the urothelial lining for signs of damage or inflammation. To add on, a long-term risk evaluation of stent-related symptoms such as encrustation and bacterial infection could also be performed. Finally, the current work only evaluates

the coated device in healthy porcine ureter, hence only a preliminary single swollen hydrogel stent section (7 mm) is used. Future work will involve the creation of stricture in target ureteric segment in which ureteric dilation is expected to be less due to the fibrosis present. Stents coated with hydrogel that swells to varying diameter sizes will be implanted to evaluate device safety and efficacy to manage stricture.

Conflict of interest

No conflict of interest.

Patent

WO2016148648 A1.A Stent Assembly and Method of Preparing the Stent Assembly. Filed on March 15, 2016.

Acknowledgements

This research is funded by Singapore Ministry of Education (MOE) Academic Research Fund (AcrF) Tier 1 Grant and the Singapore Ministry of Health's National Medical Research Council through the National Health Innovation Centre Singapore under its Innovation to Develop Grant (NHIC-I2D-1506051).

References

[1] Yossepowitch O, Lifshitz DA, Dekel Y, Ehrlich Y, Gur U, Margel D, et al. Assessment of vesicoureteral reflux in patients with self-retaining ureteral stents: implications for upper urinary tract instillation. The Journal of urology. 2005;173:890-3.
[2] Roberts WW, Cadeddu JA, Micali S, Kavoussi LR, Moore RG. Ureteral stricture formation after removal of impacted calculi. The Journal of urology. 1998;159:723-6.
[3] Wolf JS, Jr., Elashry OM, Clayman RV. Long-term results of endoureterotomy for benign ureteral and ureteroenteric strictures. The Journal of urology. 1997;158:759-64.
[4] Ali L, Shahzad M, Orakzai N, Khan I, Ahmad M. Efficacy of mitomycin C in reducing recurrence of anterior urethral stricture after internal optical urethrotomy. Korean Journal of Urology. 2015;56:650-5.
[5] El-Asmar KM, Hassan MA, Abdelkader HM, Hamza AF. Topical mitomycin C application is effective in management of localized caustic esophageal stricture: a double-blinded, randomized, placebo-controlled trial. Journal of pediatric surgery. 2013;48:1621-7.
[6] Huang YY, Venkatraman SS, Boey FYC, Lahti EM, Umashankar PR, Mohanty M, et al. In vitro and in vivo performance of a dual drug-eluting stent (DDES). Biomaterials. 2010;31:4382-91.
[7] Huang Y, Venkatraman SS, Boey FY, Umashankar PR, Mohanty M, Arumugam S. The short-term effect on restenosis and thrombosis of a cobalt-chromium stent eluting two drugs in a porcine coronary artery model. J Interv Cardiol. 2009;22:466-78.

[8] Huang Y, Ng HC, Ng XW, Subbu V. Drug-eluting biostable and erodible stents. J Control Release. 2014;193:188-201.
[9] Huang Y, Ng XW, Lim SG, Chen HH, Burnett JC, Jr., Boey YC, et al. In vivo Evaluation of Cenderitide-Eluting Stent (CES) II. Annals of biomedical engineering. 2016;44:432-41.
[10] Ang HY, Bulluck H, Wong P, Venkatraman SS, Huang Y, Foin N. Bioresorbable stents: Current and upcoming bioresorbable technologies. International Journal of Cardiology.228:931-9.
[11] Kallidonis P, Kitrou P, Karnabatidis D, Kyriazis I, Kalogeropoulou C, Tsamandas A, et al. Evaluation of zotarolimus-eluting metal stent in animal ureters. Journal of endourology. 2011;25:1661-7.
[12] Lin JS-J, Kleinmann N, Wirth GJ, Matin SF, Mayer G, Nativ O, et al. Thermo reversible hydrogel based delivery of mitomycin C for treatment of upper tract urothelial carcinoma (UTUC). Journal of Clinical Oncology. 2017;35:e16089-e.
[13] Mendez-Probst CE, Goneau LW, MacDonald KW, Nott L, Seney S, Elwood CN, et al. The use of triclosan eluting stents effectively reduces ureteral stent symptoms: a prospective randomized trial. Bju International. 2012;110:749-54.
[14] Krambeck AE, Walsh RS, Denstedt JD, Preminger GM, Li J, Evans JC, et al. A novel drug eluting ureteral stent: a prospective, randomized, multicenter clinical trial to evaluate the safety and effectiveness of a ketorolac loaded ureteral stent. The Journal of urology. 2010;183:1037-42.
[15] Barros AA, Oliveira C, Lima E, Duarte ARC, Healy K, Reis RL. 7.41 Ureteral Stents Technology: Biodegradable and Drug-Eluting Perspective A2 - Ducheyne, Paul. Comprehensive Biomaterials II. Oxford: Elsevier; 2017. p. 793-812.
[16] Barros AA, Browne S, Oliveira C, Lima E, Duarte ARC, Healy KE, et al. Drug-eluting biodegradable ureteral stent: New approach for urothelial tumors of upper urinary tract cancer. International Journal of Pharmaceutics. 2016;513:227-37.
[17] Barros AA, Oliveira C, Reis RL, Lima E, Duarte ARC. In Vitro and Ex Vivo Permeability Studies of Paclitaxel and Doxorubicin From Drug-Eluting Biodegradable Ureteral Stents. Journal of Pharmaceutical Sciences. 2017;106:1466-74.
[18] Hurst RE, Greenwood-Van Meerveld B, Wisniewski AB, VanGordon S, Lin H, Kropp BP, et al. Increased bladder permeability in interstitial cystitis/painful bladder syndrome. Translational Andrology and Urology. 2015;4:563-71.
[19] Apodaca G. The uroepithelium: not just a passive barrier. Traffic (Copenhagen, Denmark). 2004;5:117-28.
[20] Khandelwal P, Abraham SN, Apodaca G. Cell biology and physiology of the uroepithelium. American journal of physiology Renal physiology. 2009;297:F1477-501.
[21] Kreft ME, Hudoklin S, Jezernik K, Romih R. Formation and maintenance of blood-urine barrier in urothelium. Protoplasma. 2010;246:3-14.
[22] Hu P, Meyers S, Liang FX, Deng FM, Kachar B, Zeidel ML, et al. Role of membrane proteins in permeability barrier function: uroplakin ablation elevates urothelial permeability. American journal of physiology Renal physiology. 2002;283:F1200-7.
[23] Tyagi P, Wu P-C, Chancellor M, Yoshimura N, Huang L. Recent Advances in Intravesical Drug/Gene Delivery. Molecular pharmaceutics. 2006;3:369-79.

[24] Xiong GM, Ang H, Lin J, Lui YS, Phua JL, Chan JN, et al. Materials technology in drug eluting balloons: Current and future perspectives. Journal of Controlled Release. 2016;239:92-106.
[25] Ang H, Lin J, Huang YY, Chong TT, Cassese S, Joner M, et al. Drug-Coated Balloons: Technologies and Clinical Applications. Curr Pharm Des. 2017.
[26] Liourdi D, Kallidonis P, Kyriazis I, Tsamandas A, Karnabatidis D, Kitrou P, et al. Evaluation of the distribution of Paclitaxel by immunohistochemistry and nuclear magnetic resonance spectroscopy after the application of a drug-eluting balloon in the porcine ureter. Journal of endourology. 2015;29:580-9.
[27] Yang S-H, Lee Y-SJ, Lin F-H, Yang J-M, Chen K-s. Chitosan/poly(vinyl alcohol) blending hydrogel coating improves the surface characteristics of segmented polyurethane urethral catheters. Journal of Biomedical Materials Research Part B: Applied Biomaterials. 2007;83B:304-13.
[28] Chevalier RP, Ernster CJ. Ureteral stents, drainage tubes and the like. Google Patents; 1994.
[29] Lee BH, Kim MH, Lee JH, Seliktar D, Cho NJ, Tan LP. Modulation of Huh7.5 spheroid formation and functionality using modified PEG-based hydrogels of different stiffness. PloS one. 2015;10:e0118123.
[30] Wong YS, Salvekar AV, Zhuang KD, Liu H, Birch WR, Tay KH, et al. Bioabsorbable radiopaque water-responsive shape memory embolization plug for temporary vascular occlusion. Biomaterials. 2016;102:98-106.
[31] Venkatraman S, HUANG Y, LIM WS, Chong TW. A stent assembly and method of preparing the stent assembly. Google Patents; 2016.
[32] S Venkatraman XY, H Yingying, D Mondal, LK Lin. Bioactive coatings for implanted devices. In: Zhang S, editor. Biological and Biomedical Coatings Handbook: Applications: CRC Press; 2016. p. 471.
[33] Cummings LJ, Waters SL, Wattis JA, Graham SJ. The effect of ureteric stents on urine flow: reflux. Journal of mathematical biology. 2004;49:56-82.
[34] Siggers JH, Waters S, Wattis J, Cummings L. Flow dynamics in a stented ureter. Mathematical medicine and biology : a journal of the IMA. 2009;26:1-24.
[35] Wolf JS, Jr., Humphrey PA, Rayala HJ, Gardner SM, Mackey RB, Clayman RV. Comparative ureteral microanatomy. Journal of endourology. 1996;10:527-31.
[36] Luong PT, Browning MB, Bixler RS, Cosgriff-Hernandez E. Drying and storage effects on poly(ethylene glycol) hydrogel mechanical properties and bioactivity. Journal of biomedical materials research Part A. 2014;102:3066-76.
[37] Clavica F, Zhao X, ElMahdy M, Drake MJ, Zhang X, Carugo D. Investigating the Flow Dynamics in the Obstructed and Stented Ureter by Means of a Biomimetic Artificial Model. PloS one. 2014;9:e87433.
[38] Wong RS, Ashton M, Dodou K. Effect of Crosslinking Agent Concentration on the Properties of Unmedicated Hydrogels. Pharmaceutics. 2015;7:305-19.
[39] Landgraf R, Kaiser MK, Posseckardt J, Adolphi B, Fischer WJ. Functionalization of Polymer Sensor Surfaces by Oxygen Plasma Treatment. Procedia Chemistry. 2009;1:1015-8.
[40] Vlachopoulou M-E, Kokkoris G, Cardinaud C, Gogolides E, Tserepi A. Plasma Etching of Poly(dimethylsiloxane): Roughness Formation, Mechanism, Control, and

Application in the Fabrication of Microfluidic Structures. Plasma Processes and Polymers. 2013;10:29-40.
[41] Hanefeld P, Westedt U, Wombacher R, Kissel T, Schaper A, Wendorff JH, et al. Coating of Poly(p-xylylene) by PLA-PEO-PLA Triblock Copolymers with Excellent Polymer−Polymer Adhesion for Stent Applications. Biomacromolecules. 2006;7:2086-90.
[42] Riau AK, Mondal D, Yam GHF, Setiawan M, Liedberg B, Venkatraman SS, et al. Surface Modification of PMMA to Improve Adhesion to Corneal Substitutes in a Synthetic Core–Skirt Keratoprosthesis. ACS Applied Materials & Interfaces. 2015;7:21690-702.
[43] Lee C, Rasiah I, Chai TC, Gopalakrishnan R. The role of surface morphology on interfacial adhesion in IC packaging. Proceedings of the 1997 1st Electronic Packaging Technology Conference (Cat No97TH8307)1997. p. 201-7.
[44] Baker R, Baker RW. Controlled release of biologically active agents: Wiley; 1987.
[45] Hsu S-T, Yao YL. Effect of drug loading and laser surface melting on drug release profile from biodegradable polymer. Journal of Applied Polymer Science. 2013;130:4147-56.
[46] Peng Y, Ang M, Foo S, Lee WS, Ma Z, Venkatraman SS, et al. Biocompatibility and Biodegradation Studies of Subconjunctival Implants in Rabbit Eyes. PloS one. 2011;6:e22507.
[47] Fu Y, Kao WJ. Drug Release Kinetics and Transport Mechanisms of Non-degradable and Degradable Polymeric Delivery Systems. Expert opinion on drug delivery. 2010;7:429-44.
[48] Fritz JL, Owen MJ. Hydrophobic Recovery of Plasma-Treated Polydimethylsiloxane. The Journal of Adhesion. 1995;54:33-45.
[49] Pimenta AF, Valente A, Pereira JM, Pereira JC, Filipe HP, Mata JL, et al. Simulation of the hydrodynamic conditions of the eye to better reproduce the drug release from hydrogel contact lenses: experiments and modeling. Drug delivery and translational research. 2016;6:755-62.
[50] Bajgrowicz M, Phan CM, Subbaraman LN, Jones L. Release of Ciprofloxacin and Moxifloxacin From Daily Disposable Contact Lenses From an In Vitro Eye Model. Investigative ophthalmology & visual science. 2015;56:2234-42.
[51] Ali M, Horikawa S, Venkatesh S, Saha J, Hong JW, Byrne ME. Zero-order therapeutic release from imprinted hydrogel contact lenses within in vitro physiological ocular tear flow. Journal of controlled release : official journal of the Controlled Release Society. 2007;124:154-62.
[52] Huang Y-y, Qi M, Zhang M, Liu H-z, Yang D-z. Degradation mechanisms of poly (lactic-co-glycolic acid) films in vitro under static and dynamic environment. Transactions of Nonferrous Metals Society of China. 2006;16:s293-s7.
[53] Lele BS, Hoffman AS. Mucoadhesive drug carriers based on complexes of poly(acrylic acid) and PEGylated drugs having hydrolysable PEG-anhydride-drug linkages. Journal of controlled release : official journal of the Controlled Release Society. 2000;69:237-48.
[54] Laube N, Desai C, Bernsmann F, Fisang C. Ureteral stents should be soaked for several minutes before placement. SpringerPlus. 2015;4:247.

[55] Payne SR, Ramsay JW. The effects of double J stents on renal pelvic dynamics in the pig. The Journal of urology. 1988;140:637-41.
[56] Dalton JT, Wientjes MG, Badalament RA, Drago JR, Au JL. Pharmacokinetics of intravesical mitomycin C in superficial bladder cancer patients. Cancer research. 1991;51:5144-52.
[57] Samra M, Abcar AC. False Estimates of Elevated Creatinine. The Permanente Journal. 2012;16:51-2.
[58] Will TA, Polcari AJ, Garcia JG, Ouwenga MK, Voelzke BB, Greisler HP, et al. Paclitaxel inhibits ureteral smooth muscle cell proliferation and collagen production in the absence of cell toxicity. The Journal of urology. 2011;185:335-40.